

# Sapphirine and Ti-clinohumite in ultra-high-pressure garnet-pyroxenite and eclogite from Dabie Shan, China

Aral I. Okay

İTÜ, Maden Fakültesi, Jeoloji Bölümü, Ayazağa, İstanbul, Turkey

Received May 18, 1993 / Accepted September 15, 1993

**Abstract.** Sapphirine occurs as inclusions along with clinocllore, enstatite, talc, corundum, gedrite, hornblende and phlogopite in millimetre-size garnets from the orthopyroxenites in a 50-m-thick mafic-ultramafic lens in Dabie Shan in China. The lens, enclosed by felsic gneiss, is made up of metre-scale intercalation of garnet-orthopyroxenite, garnet-clinopyroxenite, eclogite and gneiss. The equilibrium conditions of the matrix minerals, as determined from the Fe-Mg exchange equilibria between garnet and orthopyroxene, and Al solubility in orthopyroxene were  $740 \pm 50^\circ\text{C}$  temperature and over 40 kbar pressure. Pressures of over 28 kbar are also indicated by inclusions of quartz pseudomorphs after coesite in garnet from the eclogites. Phase relations among the inclusion minerals, on the other hand, indicate similar temperatures of  $730 \pm 30^\circ\text{C}$  but much lower pressures of  $4 \pm 2$  kbar. The mafic-ultramafic lens was therefore not a direct mantle fragment but was probably a low-pressure cumulate in the upper crust. The early granulite-facies metamorphism was most likely part of a Precambrian event genetically unrelated to the Triassic ultra-high-pressure metamorphism. Ti-clinohumite occurs in garnet-orthopyroxenites as a matrix mineral and appears to have been stable during the ultra-high-pressure metamorphism. Its stability was controlled by the fluorine fugacity as documented by its reaction textures with olivine.

## Introduction

Sapphirine is a characteristic mineral for the granulite-facies metamorphism of magnesium- and aluminium-rich and calcium-poor rocks, and is frequently associated with orthopyroxene, cordierite and sillimanite. Here, I describe sapphirine along with enstatite, clinocllore, gedrite, corundum and talc as inclusions in garnet from a pyroxenite-eclogite lens from the ultra-high-pressure metamorphic terrain of Dabie Shan. The presence of sap-

phirine provides tight constraints on the early *P-T* evolution of the ultra-high-pressure metamorphic rocks.

Another interesting mineral that occurs in the same outcrop with sapphirine is Ti-clinohumite. Ti-clinohumite has a composition similar to olivine but contains hydroxyl groups in its structure and is therefore considered as a possible site for water in the mantle (McGetchin et al. 1970). Although it is described from kimberlites (Aoki et al. 1976), its relevance as a high-pressure phase in these heterogeneous rocks is debated (Smith 1977). It is relatively common in the Alpine antigorite-serpentinites as a secondary mineral and breaks down to olivine and ilmenite at temperatures as low as  $520^\circ\text{C}$  (Trommsdorff and Evans 1980). However, its thermal stability increases through the substitution of OH by F, as confirmed by the experimental work of Engi and Lindsley (1980). In accordance with this, Evans and Trommsdorff (1983) described F-bearing Ti-clinohumite in association with olivine and orthopyroxene and inferred it to be part of the garnet-lherzolite mineral assemblage. In the investigated pyroxenite-eclogite lens, Ti-clinohumite-bearing garnet-orthopyroxenites are interlayered on a metre scale with eclogites thus providing further constraints on the *P-T* stability of the Ti-clinohumite.

## Geological setting

The sapphirine and Ti-clinohumite-bearing rocks occur within the Dabie Shan Complex in the eastern part of the Qinling orogen in China (Fig. 1). The Dabie Shan Complex is a 150-km-wide gneiss-granite belt that consists of several tectonic slices with different metamorphic and structural features all intruded by voluminous Mesozoic granitic bodies (Okay et al. 1993). One such slice is the eclogite zone, made up of granoblastic, felsic gneiss with eclogite lenses and bands, and marble layers with calcium-rich eclogite boudins and rare ultramafic-eclogite bodies. Coesite and diamond occur as inclusions in garnet and pyroxene in the eclogites (Okay et al. 1989; Wang et al. 1989; Xu et al. 1992). A Triassic regional ultra-high-pressure metamorphism is suggested for the eclogite zone based on the geochronology and petrology of the eclogite, calc-silicate rock and gneiss (Okay et al. 1989; Okay 1993). The eclogite zone forms a 20-km-thick regularly south dipping gneiss-

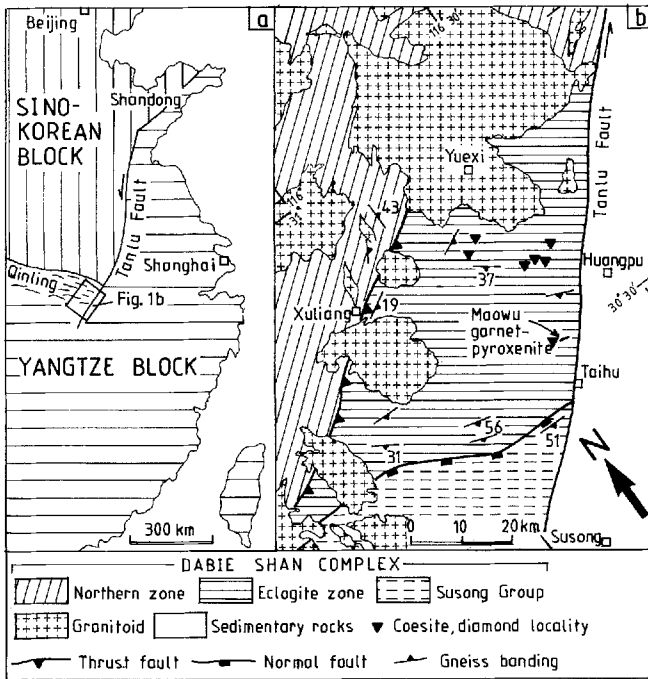


Fig. 1. **a** Tectonic map of eastern China showing the location of the studied area. **b** Tectonic map of the Dabie Shan region; the investigated Maowu body is indicated

rich sequence that is tectonically sandwiched between two amphibolite-facies slices (the northern zone and the Susong group of Fig. 1). It includes metres-thick and ten-metres long ultramafic lenses, which make up less than 1% of the whole sequence and are mostly antigorite-serpentinites. One exception is the sapphirine- and Ti-clinohumite-bearing Maowu body that consists of fresh garnet-pyroxenite and eclogite.

### Field relations

The Maowu pyroxenite-eclogite body forms an irregular lens, 210 m long and 50 m thick, in the granoblastic felsic gneisses 9 km north of Taihu (Fig. 1, lat. 30°30'00" N, long. 116°18'20" E). A map and cross-section of the body are given in Figs. 3 and 4 of Wang et al. (1990); however, unlike Wang et al. (1990) no serpentinite or peridotite was observed in the field or in the samples collected. The Maowu body is well exposed in a small disused quarry where it is seen to consist of metre-scale intercalations of garnet-orthopyroxenite, garnet-clinopyroxenite, eclogite and gneiss (Fig. 2). The inter-

nal fabric of the pale olive-green garnet-orthopyroxenite layers is defined by centimetre-scale, red garnet-rich bands, while there is millimetre-scale streaky banding in the garnet-clinopyroxenite and eclogite layers defined by variable concentrations of bright green clinopyroxene and red garnet. Very friable felsic gneiss bands with talc- and chlorite-rich reaction zones are intercalated in the sequence.

### Petrography

The three main rock types in the Maowu body, garnet-orthopyroxenite, garnet-clinopyroxenite and eclogite, show a well-developed granoblastic polygonal metamorphic fabric and most are very fresh. Typical mineral assemblages and modal amounts of these rock types are listed in Table 1.

### Orthopyroxenite

The matrix mineral assemblage in the orthopyroxenite is enstatite + garnet + chlorite ± Ti-clinohumite ± diopside ± magnesite ± olivine ± rutile. Chlorite, enstatite, sapphirine, gedrite, hornblende, talc, rutile, phlogopite, corundum and zircon occur, in decreasing order of abundance, as small inclusions in garnet (Fig. 3a–d, Table 1).

Enstatite generally makes up the bulk of the orthopyroxenites and forms a polygonal mosaic of 1–3 mm large grains with well-developed triple junctions. Garnet is a minor phase in Ti-clinohumite-bearing samples and locally occurs as inclusions in enstatite (Fig. 3e). In garnet-rich bands, garnet makes up to 60 modal% of the rock and forms millimetre-diameter sub-idioblastic grains with large number of irregularly shaped, small (< 0.02 mm) inclusions that tend to cluster in the garnet cores (Fig. 3a–d). Chlorite occurs both as a matrix phase and as common inclusions in garnet and enstatite, either as a single phase or in composite inclusions with sapphirine, gedrite, hornblende, phlogopite and talc; chlorite is colourless and exhibits unexpectedly up to first order pink interference colours ( $\delta = 0.018$ ). Ti-clinohumite is found in two garnet-poor orthopyroxenites as millimetre-size, zoned, reddish-brown crystals with lamellar or rounded Cr-spinel inclusions. In one sample (568P) it exhibits textural equilibrium with enstatite and garnet

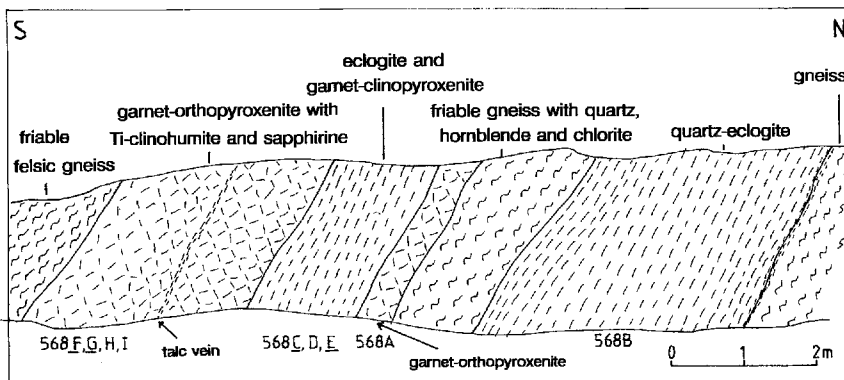


Fig. 2. Field cross-section of the western wall of the quarry in the Maowu body showing the specimen locations; the analysed samples are underlined; the rest of the samples are taken from the eastern wall of the quarry. Notice the metre-scale interlayering of different lithologies

**Table 1.** Estimated modes of the analysed samples

	Orthopyroxenite				Clinopyroxenite		Eclogite
	568F	568G	568P	568J	568E	568K	568C
Garnet	36	tr <sub>i</sub>	4	58	58	61	52
Enstatite	63	90	78	26	—	—	—
Diopside	—	—	—	15	41	38	—
Omphacite	—	—	—	—	—	—	47
Ti-clinohumite	—	5	5	—	—	—	—
Olivine	—	2	tr <sub>i</sub>	—	—	—	—
Chlorite	tr	1	—	tr	tr <sub>i</sub>	tr	—
Sapphirine	tr <sub>i</sub>	—	—	tr <sub>i</sub>	—	—	—
Talc	tr <sub>i</sub>	—	—	tr <sub>i</sub>	—	—	—
Gedrite	tr <sub>i</sub>	—	—	tr <sub>i</sub>	—	—	—
Hornblende	tr <sub>i</sub>	—	—	tr <sub>i</sub>	—	—	—
Phlogopite	—	—	—	tr <sub>i</sub>	—	tr <sub>i</sub>	—
Corundum	—	—	—	tr <sub>i</sub>	—	—	—
Epidote	—	—	—	—	—	tr <sub>i</sub>	—
Magnesite	—	—	11	—	—	—	—
Cr-spinel	—	2	2	—	—	—	—
Rutile	tr	—	—	tr	1	tr	1
Ilmenite	—	tr <sub>i</sub>	—	—	—	1	—
Pyrite	—	tr <sub>i</sub>	—	—	—	—	—

tr < 1%; i, phases that occur only as inclusions; zircon is present in all samples in trace amounts

(Fig. 3e), while in the other sample it topotactically replaces olivine (Fig. 3g). *Cr-spinel* occurs in the matrix as sub-idioblastic opaque grains and as inclusions in Ti-clinohumite. *Olivine* exhibits three modes of occurrence. It forms small inclusions in enstatite (Fig. 3e), makes up clear matrix grains that are topotactically being replaced by Ti-clinohumite (Fig. 3g) and occurs as crystals full of *magnesian-ilmenite* inclusions and with small brown patches of Ti-clinohumite (Fig. 3f). Such ilmenite-charged olivines are typical breakdown products of Ti-clinohumite (Trommsdorff and Evans 1980). *Diopside* occurs in one sample coexisting with garnet and enstatite (Table 1). *Magnesite* is a primary matrix phase associated with enstatite, Ti-clinohumite and garnet. *Sapphirine* is found as colourless inclusions in garnet, either on its own or with hornblende or chlorite. *Gedrite* and *hornblende* occur generally as colourless individual inclusions; however, composite inclusions of gedrite + chlorite, hornblende + chlorite or gedrite + talc are also present. *Talc* is usually found together with chlorite or more rarely with gedrite as composite inclusions in garnet. *Phlogopite* occurs as colourless inclusions usually with chlorite in which case they both share a common cleavage plane. *Pyrite* is rare.

#### Clinopyroxenite

The mineral assemblage in the clinopyroxenite is garnet + diopside + chlorite + rutile ± ilmenite. Millimetre-size garnet and diopside grains form a granoblastic matrix. Garnets have abundant diopside, chlorite, phlogopite and epidote inclusions.

#### Eclogite

Eclogites with garnet + omphacite + rutile are texturally similar to the garnet-clinopyroxenites; rare quartz-eclogite layers composed of garnet, very fine grained diopside + plagioclase symplectite after omphacite; quartz, kyanite, zoisite and biotite + feldspar pseudomorphs after phengite are also present (Fig. 2). The garnets from the quartz-eclogite contain cryptocrystalline quartz aggregates with radial fractures around them interpreted as pseudomorphs after coesite, which are also recorded by Wang et al. (1990).

#### Gneiss

The felsic gneiss consists of quartz, plagioclase, epidote, green hornblende, biotite and sphene. In mineral assemblage and texture it is similar to the felsic gneisses that make up the bulk of the eclogite zone (Okay et al. 1993).

#### Analytical method

Seven samples from the Maowu body were analysed with a SX-50 Cameca electron microprobe in the Department of Earth Sciences in Cambridge, England. The operating conditions were 20 kV accelerating voltage, 10 nA beam current and 10 µm beam size. The elements were analysed with energy dispersive spectrometers except for fluorine, where wavelength dispersive spectrometers were used.

The *P-T* locations of mineral reactions were calculated using the THERMOCALC programme of Holland and Powell (1990). As almost all the analysed mineral compositions are close to the Mg-endmembers, activities were calculated assuming ideal-mixing-on-sites.

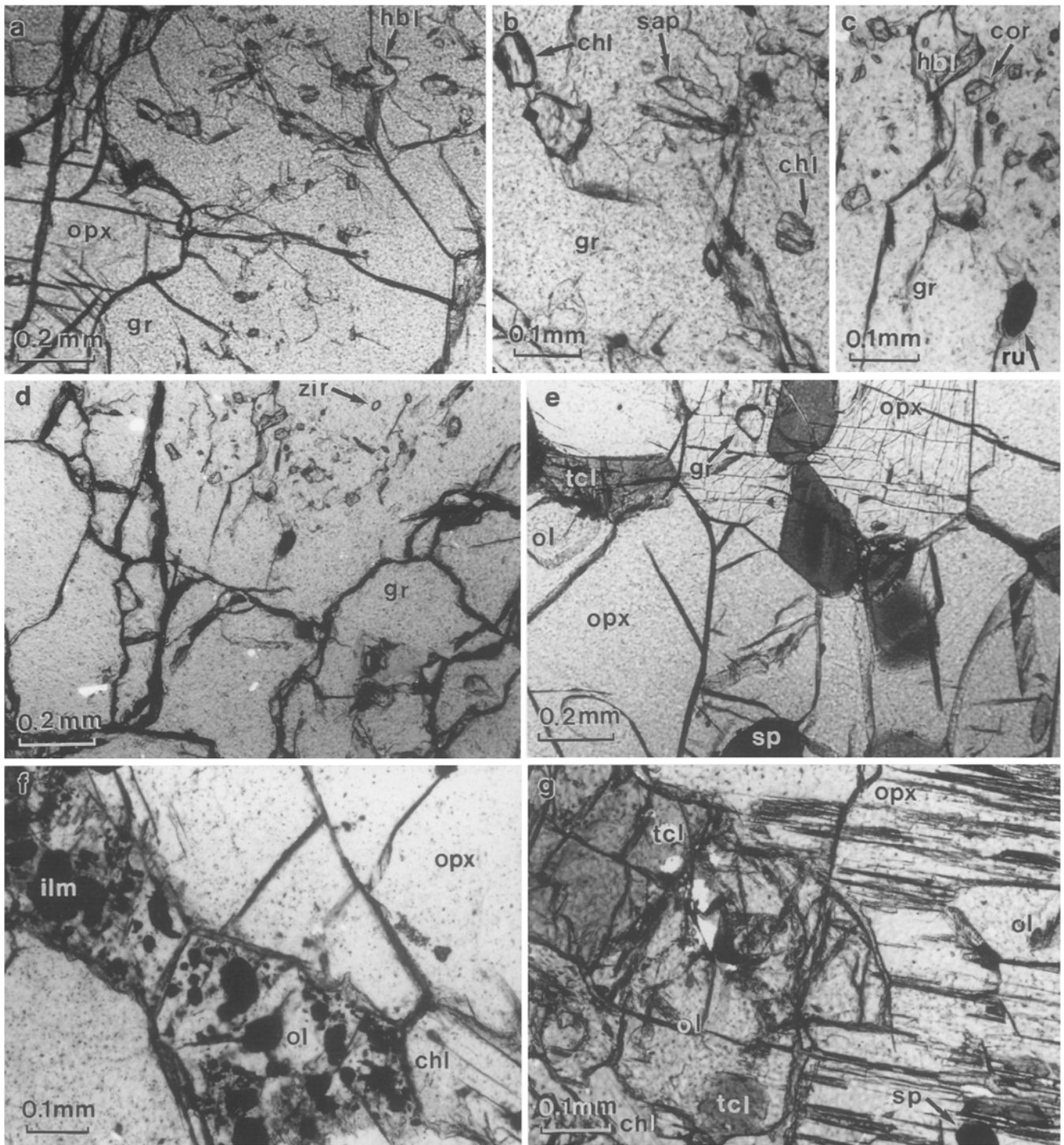


**Fig. 3a-g.** Photomicrographs in plane polarised light from the Maowu body. **a** Garnet-orthopyroxenite (568F) with enstatite, *opx*, and poikilitic garnet, *gr*. **b** Enlarged view of the poikilitic garnet, *gr*, in **a** with chlorite, *chl*, and sapphirine, *sap*, inclusions. **c** Hornblende, *hbl*, corundum, *cor*, and rutile, *ru*, inclusions in garnet, *gr*, from orthopyroxenite (568J) **d** Large poikilitic garnet from orthopyroxenite (568J) with hornblende, corundum, zircon, *zir*, inclusions. No-

tice the inclusion-free rim. An enlarged view of the garnet core is shown in **c**. **e** Ti-clinohumite, *tcl*, in textural equilibrium with enstatite, *opx*, and Cr-spinel, *sp*, from the garnet-orthopyroxenite (568P). Enstatite contains small garnet, *gr*, and olivine, *ol*, inclusion. **f** Olivine, *ol*, with Mg-ilmenite inclusions, *ilm*, after Ti-clinohumite in garnet-pyroxenite (568G). **g** Ti-clinohumite, *tcl*, topotactically replacing olivine, *ol*, in garnet-pyroxenite (568G)

## Mineral chemistry

### Garnet

The pyrope content of the garnet increases from about 53 mol% in eclogite through 60–71 mol% in clinopyroxenite to 69–75 mol% in orthopyroxenite (Fig. 4, Table 2). Uvarovite and andradite contents are appreciable in orthopyroxenite (10 and 3 mol% respectively), while they are below 1% in the clinopyroxenite and eclogite. Grossular contents are 8–12 mol% in eclogite and clinopyroxenite while they are less than 3 mol% in orthopyroxenite. Spessartine contents are around 1 mol%. Garnet is compositionally homogeneous and even the largest garnets do not show any zoning (Fig. 4).

### Orthopyroxene

The enstatite is not zoned and shows a narrow range of composition with Mg values [ $100\text{Mg}/(\text{Fe} + \text{Mg})$ ] of 92 to 94 (Table 2). The  $\text{Al}_2\text{O}_3$  contents of the matrix enstatites are below the detection limit of the electron probe while some of the enstatite inclusions in garnet contain up to 0.12 wt%  $\text{Al}_2\text{O}_3$ . The CaO contents of the enstatite range from 0.00 to 0.08 wt%.

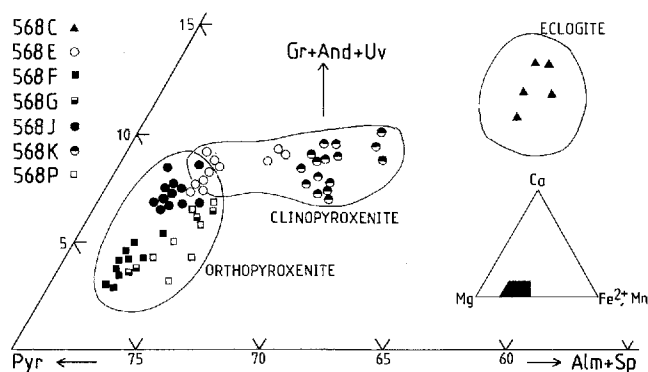


**Fig. 4.** Garnet compositions from the Maowu body shown in part of the garnet ternary compositional field. The inset shows the setting of the enlarged area within the garnet ternary field. *Gr*, grossular; *And*, andradite; *Uv*, uvarovite; *Pyr*, pyrope; *Alm*, almandine; *Sp*, spessartine

**Table 2.** Representative mineral analyses from the Maowu body

	Garnet							Orthopyroxene			Clinopyroxene			
	568C	568E	568F	568G inc	568J	568K	568P	568G	568F	568J	568C	568E	568J	568K
SiO <sub>2</sub>	40.73	41.59	41.99	41.75	41.87	40.76	40.90	58.53	58.47	58.37	56.58	55.50	54.93	55.04
TiO <sub>2</sub>	0.05	0.07	0.04	0.00	0.00	0.01	0.00	0.01	0.00	0.00	0.07	0.06	0.00	0.00
Al <sub>2</sub> O <sub>3</sub>	22.76	23.50	23.46	21.80	23.09	22.07	20.95	0.00	0.00	0.00	10.21	1.35	1.17	0.38
Cr <sub>2</sub> O <sub>3</sub>	0.07	0.05	0.14	1.76	0.28	0.76	3.44	0.02	0.15	0.00	0.10	0.21	0.34	0.31
FeO	16.99	12.47	11.86	12.63	11.91	15.57	11.84	5.22	5.40	5.56	3.11	2.35	2.03	2.40
MgO	14.77	19.21	21.19	19.62	19.75	16.90	19.32	36.32	35.92	35.91	9.68	16.75	16.77	17.43
MnO	0.40	0.41	0.46	0.49	0.35	0.46	0.59	0.13	0.01	0.03	0.04	0.00	0.06	0.14
CaO	4.14	3.41	1.49	2.45	2.90	3.68	2.47	0.07	0.07	0.08	13.84	22.83	22.92	23.54
Na <sub>2</sub> O	0.04	0.09	0.00	0.00	0.11	0.00	0.02	0.00	0.19	0.06	6.97	1.37	1.53	0.93
K <sub>2</sub> O	0.00	0.00	0.02	0.01	0.00	0.01	0.01	0.00	0.03	0.00	0.01	0.01	0.02	0.09
Total	99.95	100.80	100.65	100.51	100.26	100.22	99.54	100.30	100.24	100.01	100.61	100.43	99.77	100.26
Formula based on:														
	12 ox	12 ox	12 ox	12 ox	12 ox	12 ox	12 ox	6 ox	6 ox	6 ox	4 cat	4 cat	4 cat	4 cat
Si	2.999	2.970	2.978	3.000	2.994	2.982	2.978	1.998	1.999	2.000	1.982	1.993	1.982	1.985
Al <sup>4</sup>	0.001	0.030	0.022	0.000	0.006	0.018	0.022	0.000	0.000	0.000	0.018	0.007	0.018	0.015
Al <sup>6</sup>	1.974	1.948	1.940	1.846	1.940	1.886	1.776	0.000	0.000	0.000	0.404	0.050	0.031	0.001
Ti	0.003	0.004	0.002	0.000	0.000	0.000	0.000	0.000	0.000	0.000	0.002	0.002	0.000	0.000
Cr	0.004	0.003	0.008	0.100	0.016	0.044	0.198	0.001	0.004	0.000	0.003	0.006	0.010	0.009
Fe <sup>3+</sup>	0.019	0.045	0.050	0.054	0.044	0.070	0.026				0.065	0.038	0.062	0.054
Fe <sup>2+</sup>	1.025	0.700	0.654	0.704	0.668	0.882	0.694	0.149	0.154	0.159	0.026	0.033	0.000	0.029
Mg	1.621	2.045	2.240	2.102	2.106	1.842	2.096	1.848	1.831	1.834	0.506	0.897	0.902	0.936
Mn	0.024	0.025	0.028	0.030	0.022	0.028	0.036	0.004	0.000	0.001	0.001	0.000	0.002	0.004
Ca	0.327	0.261	0.112	0.188	0.222	0.288	0.192	0.002	0.002	0.003	0.519	0.878	0.886	0.909
Na	0.005	0.013	0.000	0.000	0.016	0.000	0.004	0.000	0.013	0.004	0.474	0.096	0.107	0.064
K	0.000	0.000	0.002	0.002	0.000	0.002	0.002	0.000	0.001	0.000	0.000	0.000	0.001	0.004
Total	8.002	8.044	8.036	8.026	8.034	8.042	8.024	4.002	4.004	4.001	4.000	4.000	4.001	4.000
almandine	34.2	23.1	21.6	23.3	22.1	29.0	23.0		jadeite		40.4	5.0	3.1	0.1
pyrope	54.1	67.5	73.8	69.5	69.8	60.6	69.5		aegirine		6.5	3.8	6.2	5.4
spessartine	0.8	0.8	0.9	1.0	0.7	0.9	1.2		augite		53.1	91.2	90.7	94.5
g + a + u	10.9	8.6	3.7	6.2	7.4	9.5	6.4							

inc, inclusion; g, grossular, a, andradite; u, uvarovite; ox, oxygens; cat, cations

## Clinopyroxene

The clinopyroxene compositions were calculated for four cations. The jadeite content is taken to be equal to octahedral aluminium. Aegirine component equals Na-Al<sup>vi</sup>-Ti-Cr. The rest is assigned to the augite component. Diopside contains about 5 mol% each jadeite and aegirine and less than 3 mol% hedenbergite components (Table 2). The Al<sub>2</sub>O<sub>3</sub> contents of the diopside are below 1.5 wt% and the average tschermak component (Al<sup>iv</sup>) is 0.01 per formula unit (p.f.u.).

Omphacites from the sample 568C contain about 7 mol% aegirine and 40 mol% jadeite components. They are very rich in Mg with an Mg/(Fe<sup>2+</sup> + Mg) ratio of over 0.94.

## Chlorite

Chlorite is very close to clinochlore in composition with a restricted Mg value of 94 to 97 (Fig. 5, Table 3). Chlorite from the orthopyroxenes shows substitution of Al by Cr with Cr<sub>2</sub>O<sub>3</sub> contents ranging up to 3.05 wt%. The chlorite inclusions tend to be slightly richer in Al than the matrix chlorites (Fig. 5). Chlorite from the Ti-clinohumite-bearing samples contains approx. 0.5 wt% fluorine as compared to less than 0.08 wt% in the other samples (cf. Table 3).

## Ti-clinohumite

Ti-clinohumite analyses were calculated for 13 cations (Table 3). The average Si p.f.u. based on 17 analyses is 3.976 ± 0.015 suggesting a very slight Si deficiency. The TiO<sub>2</sub> ranges from 1.33 to 3.36 wt% and shows an inverse relationship with Mg + Fe + Mn + Ca (Fig. 6) as expected from the ideal structural formula of Ti-clinohumite R<sup>2+</sup><sub>8</sub>Si<sub>4</sub>O<sub>16</sub> R<sup>2+</sup><sub>1-x</sub>Ti<sub>x</sub>(OH,F)<sub>2-2x</sub>O<sub>2x</sub>. The fluorine content ranges from 0.8 to 1.3 wt% and shows no obvious relationship with the other elements (Fig. 6). The average Cr<sub>2</sub>O<sub>3</sub> content is 0.177 ± 0.035 wt%. The Mg value ranges from 90 to 93 and is the apparent cause of the colour zoning in the Ti-clinohumite with the Fe-rich parts of the grains having a darker orange-brown colour.

## Sapphirine

Sapphirine analyses were recalculated to 10 oxygens and the Fe<sup>3+</sup> was estimated following the method of Higgins et al. (1979). In the (Mg,Fe)O-(Al,Fe)<sub>2</sub>O<sub>3</sub>-SiO<sub>2</sub> diagram sapphirine from sample 568J plots close to the 7:9:3 sapphirine while those from 568F are peraluminous (cf. Schreyer and Abraham 1975). The sapphirine compositions cluster close to the line of substitution of [(Mg,Fe<sup>2+</sup>,Mn)Si] = 2[Al,Cr, Fe<sup>3+</sup>]. The Fe<sup>3+</sup> and Cr contents are below 0.07 and 0.15 p.f.u. while the Mg/(Fe<sup>2+</sup> + Mg) ratio is 0.95 to 0.98 (Table 3).

Table 3. Representative mineral analyses from the Maowu body

	Chlorite						Ti-clinohumite		Gedrite		Hornblende		Sapphirine	
	568E inc	568F inc	568G	568J	568K		568G	568P	568F inc	568J inc	568F inc	568J inc	568F inc	568J inc
SiO <sub>2</sub>	31.24	30.80	29.53	31.19	31.08	30.98	36.88	36.84	43.11	50.64	44.85	47.62	11.87	12.64
TiO <sub>2</sub>	0.00	0.07	0.00	0.12	0.01	0.06	1.77	3.16	0.00	0.05	0.04	0.20	0.00	0.03
Al <sub>2</sub> O <sub>3</sub>	19.02	18.53	21.18	16.83	18.43	18.67	0.00	0.00	21.54	12.32	16.21	12.60	64.82	64.16
Cr <sub>2</sub> O <sub>3</sub>	0.09	0.80	0.28	1.44	0.29	0.48	0.23	0.15	0.92	0.19	0.80	0.06	1.79	0.07
FeO	2.56	2.85	2.42	2.42	2.46	3.39	9.81	7.49	5.73	5.69	3.90	3.91	2.83	3.26
MgO	34.40	33.62	33.49	34.60	34.09	33.78	49.33	49.62	24.30	27.37	18.13	18.83	18.55	19.21
MnO	0.00	0.03	0.06	0.07	0.00	0.02	0.07	0.06	0.15	0.07	0.00	0.02	0.01	0.06
CaO	0.04	0.02	0.02	0.01	0.00	0.13	0.02	0.03	0.29	0.46	12.06	12.45	0.09	0.00
Na <sub>2</sub> O	0.02	0.02	0.09	0.06	0.09	0.00	0.00	0.16	2.41	1.28	1.88	0.93	0.04	0.08
K <sub>2</sub> O	0.05	0.01	0.04	0.01	0.00	0.00	0.00	0.00	0.02	0.02	0.20	0.21	0.01	0.00
F	ND	ND	0.05	0.50	ND	ND	0.89	1.05	ND	ND	ND	ND	ND	ND
Total	87.42	86.75	87.16	87.25	86.45	87.51	99.00	98.56	98.47	98.09	98.07	96.83	100.01	99.51
Formula based on:														
	14 ox	14 ox	14 ox	14 ox	14 ox	14 ox	13 cat	13 cat	23 ox	23 ox	23 ox	23 ox	10 ox	10 ox
Si	2.921	2.914	2.774	2.954	2.938	2.912	3.988	3.992	5.861	6.823	6.271	6.693	0.695	0.742
Al <sup>4</sup>	1.079	1.086	1.226	1.046	1.062	1.088	0.000	0.000	2.139	1.177	1.728	1.307	2.305	2.258
Al <sup>6</sup>	1.018	0.981	1.120	0.832	0.991	0.979	0.000	0.000	1.311	0.778	0.944	0.782	2.172	2.182
Ti	0.000	0.005	0.000	0.009	0.000	0.005	0.144	0.258	0.000	0.004	0.004	0.023	0.000	0.000
Cr	0.007	0.061	0.021	0.108	0.021	0.035	0.019	0.013	0.100	0.019	0.088	0.008	0.083	0.003
Fe <sup>3+</sup>													0.050	0.073
Fe <sup>2+</sup>	0.200	0.226	0.190	0.192	0.194	0.266	0.888	0.678	0.652	0.640	0.456	0.460	0.088	0.087
Mg	4.794	4.741	4.690	4.884	4.804	4.732	7.952	8.015	4.926	5.497	3.780	3.945	1.620	1.682
Mn	0.000	0.002	0.005	0.005	0.000	0.002	0.007	0.006	0.015	0.008	0.000	0.000	0.000	0.000
Ca	0.004	0.002	0.002	0.001	0.000	0.014	0.002	0.003	0.042	0.065	1.806	1.875	0.005	0.000
Na	0.005	0.000	0.016	0.010	0.016	0.000	0.000	0.035	0.633	0.334	0.510	0.253	0.005	0.008
K	0.005	0.000	0.004	0.001	0.000	0.000	0.000	0.000	0.004	0.000	0.035	0.038	0.002	0.000
Total	10.033	10.018	10.048	10.042	10.026	10.033	13.000	13.000	15.683	15.345	15.623	15.384	7.025	7.035
F			0.014	0.149			0.304	0.358						

inc, inclusion; ND, not determined; ox, oxygens; cat, cations

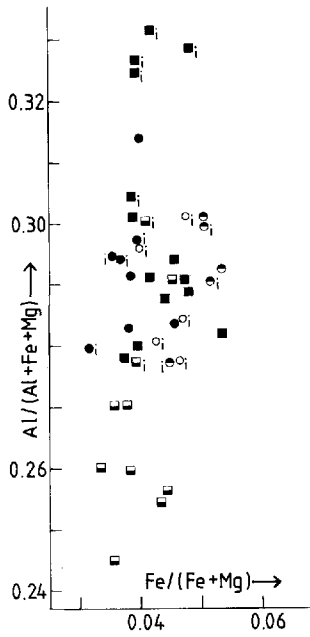


**Fig. 5.** Chlorite compositions from the Maowu body plotted in terms of their  $Fe/(Fe+Mg)$  and  $Al/(Al+Fe+Mg)$  ratios. Compositions of chlorite inclusions are denoted by *i*. The low Al values in 568G are due to Cr substituting for Al in this Cr-rich orthopyroxenite. Symbols as in Fig. 4

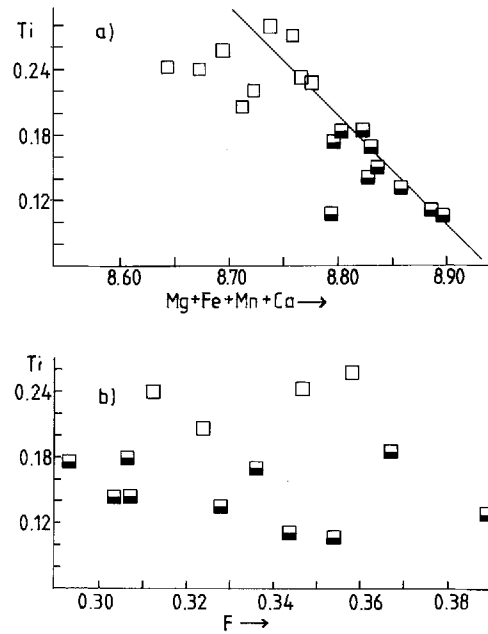


**Fig. 6a,b.** Ti-clinohumite compositions from the Maowu body shown in terms of Ti and  $(Mg+Fe+Mn+Ca)$  in 13-cation formula unit and fluorine per formula unit. **a** The line shows the ideal substitution of  $TiO_2 = (Mg,Fe,Mn,Ca)(OH,F)_2$ . Symbols as in Fig. 4

**Table 4.** Representative mineral analyses from the Maowu body

	Olivine		Corundum		Talc		Phlogopite		Epidote	Magnesite	Cr-spinel		Mg-ilmenite	
	568G	568J inc	568F inc	568J inc	568J inc	568K inc	568K inc	568K inc	568P	568G	568P	568G inc	568K inc	
SiO <sub>2</sub>	41.41	0.11	62.52	62.13	44.53	43.02	37.78	0.05	0.17	0.22	0.19	0.09		
TiO <sub>2</sub>	0.00	0.00	0.00	0.00	0.29	0.30	0.04	0.00	0.26	0.30	51.12	52.57		
Al <sub>2</sub> O <sub>3</sub>	0.00	99.71	0.23	0.10	14.71	14.41	26.53	0.00	3.98	2.69	0.03	0.10		
Cr <sub>2</sub> O <sub>3</sub>	0.03	0.19	0.07	0.05	0.01	0.04	0.16	0.00	39.97	44.65	0.46	0.48		
FeO	7.44	0.43	0.98	1.09	1.96	2.63	7.81	3.41	47.00	43.60	40.97	43.33		
MgO	51.26	0.00	30.83	30.61	26.09	25.37	0.14	46.29	5.76	5.45	6.69	4.41		
MnO	0.00	0.01	0.00	0.01	0.00	0.00	0.09	0.06	0.40	0.33	0.86	0.21		
CaO	0.00	0.06	0.00	0.01	0.01	0.02	21.91	0.12	0.01	0.00	0.00	0.09		
Na <sub>2</sub> O	0.13	0.00	0.01	0.26	0.93	0.59	0.00	0.00	0.28	0.07	0.17	0.00		
K <sub>2</sub> O	0.00	0.00	0.00	0.00	7.25	7.94	0.02	0.00	0.02	0.01	0.00	0.00		
Total	100.27	100.51	94.64	94.26	95.78	94.32	94.48	49.93	97.85	97.32	100.49	101.28		
Formula based on:														
	4 ox	3 ox	11 ox	11 ox	11 ox	11 ox	8 cat	1 cat	3 cat	3 cat	3 ox	3 ox		
Si	1.000	0.002	3.991	3.989	3.032	3.001	3.036	0.002	0.006	0.008	0.005	0.002		
Al <sup>4</sup>	0.000		0.009	0.007	0.968	0.999		0.000						
Al <sup>6</sup>	0.000	1.991	0.008		0.213	0.185	2.514	0.000	0.165	0.114	0.001	0.003		
Ti	0.000	0.000	0.000	0.000	0.015	0.017	0.002	0.000	0.007	0.008	0.938	0.963		
Cr	0.001	0.003	0.004	0.002	0.000	0.002	0.010	0.000	1.109	1.262	0.009	0.009		
Fe <sup>3+</sup>		0.006					0.525		0.726	0.624				
Fe <sup>2+</sup>	0.150		0.051	0.059	0.112	0.154		0.040	0.653	0.680	0.836	0.883		
Mg	1.845	0.000	2.933	2.930	2.647	2.638	0.017	0.955	0.302	0.289	0.243	0.160		
Mn	0.000	0.000	0.000	0.000	0.000	0.000	0.006	0.001	0.012	0.010	0.018	0.004		
Ca	0.000	0.001	0.000	0.000	0.000	0.002	1.889	0.002	0.000	0.000	0.000	0.002		
Na	0.006	0.000	0.002	0.033	0.123	0.079	0.000	0.000	0.019	0.005	0.008	0.000		
K	0.000	0.000	0.000	0.000	0.631	0.708	0.002	0.000	0.001	0.001	0.000	0.000		
Total	3.002	2.003	6.998	7.020	7.741	7.785	8.001	1.000	3.000	3.001	2.058	2.026		

inc, inclusion; ox, oxygens; cat, cations

### Other minerals

Olivine has the same composition in all its three modes of occurrence with a Mg value of 92–93 (Table 4). *Gedrite* analyses, calculated for 23 oxygens, show restricted Mg values (88–90) but relatively variable Si (5.86–6.82) and Na (0.31–0.63) contents p.f.u. (Table 3). The Na contents correlate inversely with Si implying  $\text{Na Al}^{\text{iv}} = \text{Si}$  substitution. The total for cations minus (Na+K) in the gedrite structural formula is very close to 15.00 indicating very little  $\text{Fe}^{3+}$  substitution. The *hornblende* inclusions are tschermakitic hornblende to magnesia-hornblende with Mg values of 87–90 and Na/(Ca+Na) ratios of 0.12 to 0.22 (Table 3). Gedrite and hornblende are the only minerals in the diopside-free orthopyroxenites with more than 1 wt%  $\text{Na}_2\text{O}$  and have apparently absorbed all the available Na in the rock. The composition of *talc* is close to the ideal with less than 0.5 wt%  $\text{Al}_2\text{O}_3$  and a Mg value of 96 to 98 (Table 4). *Phlogopite* is alkali deficient with Na+K p.f.u., calculated to 11 oxygens, ranging from 0.75 to 0.79 (Table 4). The Na/(K+Na) ratio ranges from 0.09 to 0.16. Silicon atoms p.f.u. total very close to 3.00 and the Mg value is 94 to 96. *Corundum* contains minor amounts of  $\text{Fe}_2\text{O}_3$  and  $\text{Cr}_2\text{O}_3$  (Table 4). *Epidote*, which is only found as inclusions in garnets from the clinopyroxenites, contains about 17 mol% pistacite component (Table 4). *Magnesite* is close to  $\text{MgCO}_3$  in composition with only 4 mol%  $\text{FeCO}_3$  and less than 0.2 mol%  $\text{CaCO}_3$  (Table 4). *Rutile* contains up to 1 wt%  $\text{Cr}_2\text{O}_3$  and 0.4 wt%  $\text{Fe}_2\text{O}_3$ . *Cr-spinels* from two Ti-clinohumite-bearing samples exhibit a narrow compositional range and are dominated by Cr and  $\text{Fe}^{3+}$  as trivalent ions and Mg,  $\text{Fe}^{2+}$  as divalent ions (Table 4). The Mg/( $\text{Fe}^{2+} + \text{Mg}$ ) ratio is about 0.30. *Magnesian-ilmenite* that occurs as inclusions in olivine contains up to 23 mol% geikielite component, while those associated with matrix chlorite have up to 18 mol% geikielite (Table 4).

The relative Mg values in the matrix minerals are garnet << olivine < Ti-clinohumite < orthopyroxene < chlorite. Diopside has appreciable ferric ion so that it is difficult to compare its Mg value with that of the other minerals.

### P-T conditions of the matrix minerals

Two  $\text{Fe}^{2+}$ -Mg exchange geothermometers are potentially applicable to Maowu rocks: garnet-clinopyroxene and garnet-orthopyroxene. The Mg-rich nature of the clinopyroxene (cf. Table 2) coupled with the uncertainties associated with the  $\text{Fe}^{3+}/\text{Fe}^{2+}$  estimation reduces the reliability of the garnet-clinopyroxene geothermometer. If all the iron in diopside is taken as ferrous, then 22 garnet-diopside pairs indicate a temperature of  $780 \pm 50^\circ\text{C}$  at 40 kbar using the calibration of Ellis and Green (1979). However, this is clearly a maximum temperature as the composition of diopside indicates that there is some aegerine component in the structure (Table 2). If the estimated ferrous iron in clinopyroxene is used for the geothermometry, then the garnet-omphacite pairs indicate a temperature of  $707 \pm 60^\circ\text{C}$ , while the garnet-diopside pairs give temperatures of  $610^\circ\text{C}$  or lower at 40 kbar.

The garnet-orthopyroxene geothermometer yields reproducible results and indicates for 13 garnet-enstatite pairs from two samples a temperature of  $740 \pm 20^\circ\text{C}$  at 40 kbar using the Harley (1984) calibration (Fig. 7). If the estimated ferrous ion rather than the total iron in garnet is used in the geothermometric calculations, then the resultant garnet-orthopyroxene temperature is about  $30^\circ\text{C}$  lower.

The enstatite content of clinopyroxene coexisting with orthopyroxene can be used as a geothermometer. In the

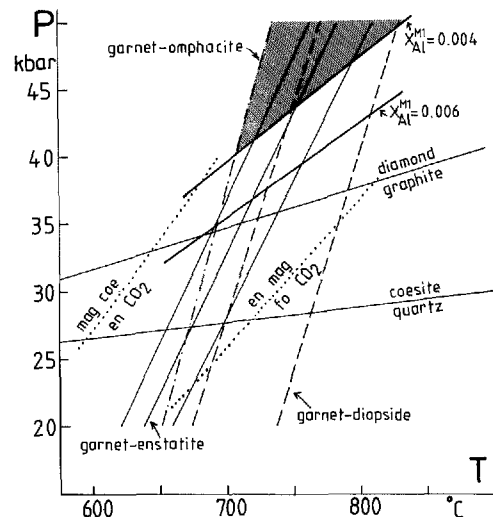


**Fig. 7.** Pressure-temperature diagram showing representative equilibria constraining the temperature and minimum pressure of the matrix minerals of the Maowu body. The garnet-omphacite and garnet-diopside (all Fe taken as  $\text{Fe}^{2+}$ ) equilibrium are after Ellis and Green (1979), the garnet-enstatite Fe-Mg equilibrium is after Harley (1984). Thick lines show garnet-enstatite Mg-Al equilibria for two hypothetical  $X_{\text{Al}}$  values for the sample 568F, providing minimum pressure brackets. The dotted lines indicate two carbonation reactions calculated by THERMOCALC for a temperature of  $740^\circ\text{C}$  and a  $X_{\text{CO}_2}$  value of 0.005. Forsterite, fo; enstatite, en; magnesite, mag; coesite, coe

sample 568J, where the two pyroxenes coexist, the Ca+Na content of the diopside is very close to 1.00 ( $>0.98$ , cf. Table 2), which results in very low and variable activities of enstatite in diopside. The highest temperature obtained from this sample using the two-pyroxene geothermometer of Wells (1977) is  $697^\circ\text{C}$ , while most clino- and orthopyroxene crystals give temperatures below  $600^\circ\text{C}$ .

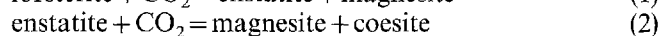
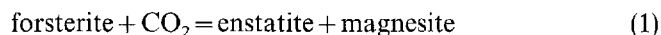
A temperature of  $740 \pm 50^\circ\text{C}$  at 40 kbar, based largely on the garnet-orthopyroxene geothermometer, is accepted as the temperature of metamorphism. A temperature below  $700^\circ\text{C}$  is unlikely on account of the absence of zoning in the garnet (e.g. Ghent 1988).

The Al-content of orthopyroxene in equilibrium with garnet decreases with increasing pressure at constant temperature and has been calibrated as a geobarometer. The  $\text{Al}_2\text{O}_3$  contents of the matrix orthopyroxenes in the Maowu body are below 0.01 wt%, indicating pressures of above 35 kbar at  $740^\circ\text{C}$  as extrapolated from the experimental work of MacGregor (1974) and Perkins et al. (1981). Taking a value of  $X_{\text{Al}}$  in orthopyroxene of 0.004, equivalent to about 0.12 wt%  $\text{Al}_2\text{O}_3$ , the Nickel and Green (1985) calibration, judged to be the best orthopyroxene-garnet geobarometer by Carswell and Gibb (1987), indicates for the sample 568F a minimum pressure of 43 kbar at  $740^\circ\text{C}$  (Fig. 7). The former presence of coesite in the quartz-eclogite gives minimum pressures of 28 kbar at  $740^\circ\text{C}$ .

Thus, the matrix minerals in the Maowu body have equilibrated at temperatures of  $740 \pm 50^\circ\text{C}$  and at pressures of above 40 kbar (Fig. 7). These pressures are well

within the stability field of diamond and are probably the highest pressures recorded as yet in rocks at such relatively low temperatures.

The fluid pressure during the ultra-high-pressure metamorphism is not constrained. However, the enstatite + magnesite assemblage in the sample 568P places constraints on the  $X_{\text{CO}_2}$  during the metamorphism through the reactions:



Both reactions occur at pressures of above 6 kbar for a wide range of  $X_{\text{CO}_2}$  values (0.001–0.9) at temperatures of above 700°C. At high-pressures these carbonation reactions occur at very low  $X_{\text{CO}_2}$  values and constrain  $X_{\text{CO}_2}$  to about 0.005 during the ultra-high-pressure metamorphism (Fig. 7). The olivine inclusions in enstatite in 568P (Fig. 3e) suggest increase in  $\text{CO}_2$  during the progressive metamorphism.

Ti-clinohumite with an average mole fraction of fluorine ( $X_{\text{F}} = \text{F}/(\text{OH} + \text{F})$ ) of 0.20–0.22 was stable during the ultra-high-pressure metamorphism as indicated by its textural equilibrium with garnet and enstatite in the sample 568P (Fig. 3e). Experimental work of Engi and Lindsley (1980) indicates that F-free Ti-clinohumite is not stable at temperatures of 700–750°C. Thus, the contrasting textures between olivine and Ti-clinohumite in the 568G (Fig. 3f,g) are caused by the variation of fluorine activity in the fluid phase. The origin of fluorine- and  $\text{CO}_2$ -bearing fluids at depths of over 100 km remain enigmatic.

### Phase relations and $P$ - $T$ conditions of the inclusion minerals

The inclusions in garnet crystals represent early phases during the progressive metamorphism as shown by the preservation of the highly unstable coesite and diamond in the cores of garnets in Dabie Shan. The early phases in the orthopyroxenites were therefore clinocllore, enstatite, sapphirine, gedrite, hornblende, talc, phlogopite and corundum. Phlogopite, gedrite and hornblende are the only major K-, Na- and Ca-bearing phases respectively so that the rest of the minerals can be represented to a close approximation in the  $\text{MgO-Al}_2\text{O}_3\text{-SiO}_2\text{-H}_2\text{O}$  system. Probable phase relations between these minerals, based on the nature of the composite inclusions, and the bulk composition of the orthopyroxenite, as approximated from the modal amounts, are shown projected from  $\text{H}_2\text{O}$  in the  $\text{MgO-SiO}_2\text{-Al}_2\text{O}_3$  diagram in Fig. 8.

The common mineral assemblage in these rocks before the formation of garnet must have been clinocllore + talc  $\pm$  sapphirine  $\pm$  enstatite (Fig. 8). The stability of the clinocllore + sapphirine is bracketed by four reactions (Fig. 9):

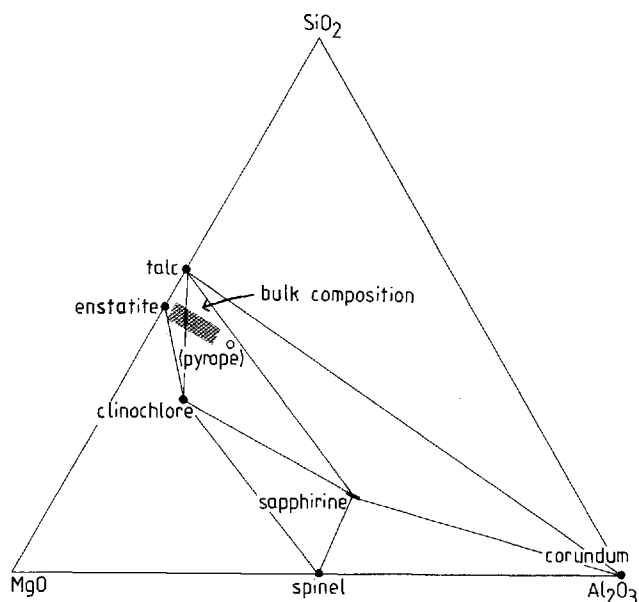
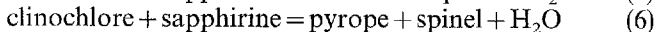
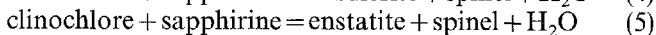
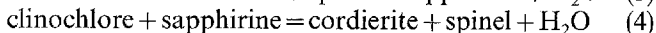
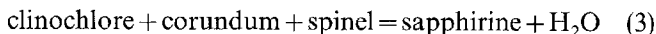


Fig. 8. Phase relations among the inclusion minerals in the Maowu body shown in the  $\text{MgO-Al}_2\text{O}_3\text{-SiO}_2$  triangle. The estimated bulk composition of the orthopyroxenite is shaded

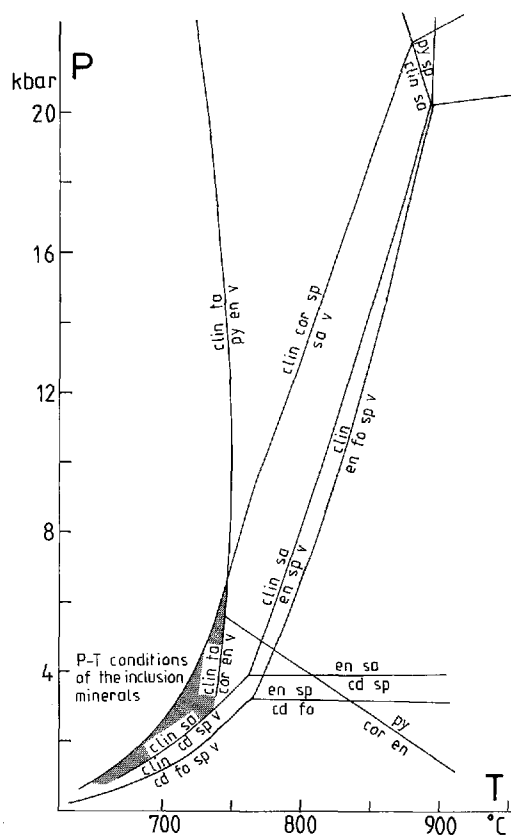
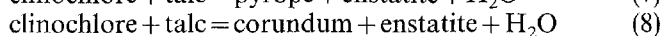
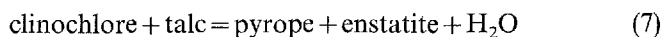


Fig. 9. Pressure-temperature diagram showing the phase equilibria constraining the  $P$ - $T$  conditions of the inclusion minerals. Reactions are based on experimental phase equilibria for endmember compositions, except those involving clinocllore + talc, and corundum + enstatite + pyrope, which were calculated for actual compositions from the sample 568J. See text for more details. Cordierite, *cd*; clinocllore, *clin*; corundum, *cor*; enstatite, *en*; forsterite, *fo*; pyrope, *py*; sapphirine, *sa*; spinel, *sp*; talc, *ta*;  $\text{H}_2\text{O}$ , *v*

The first three reactions have been experimentally determined (Seifert 1974; Ackermann et al. 1975) while the fourth reaction is readily drawn between the two experimentally determined invariant points (Staudigel and Schreyer 1977). These reactions define a 40°C-wide temperature band between 2 and 22 kbars for the stable coexistence of clinocllore and sapphirine (Fig. 9), which explains the great rarity of this assemblage in rocks.

The upper thermal stability of clinocllore + talc is defined by two dehydration reactions:



These reactions were calculated using actual compositions from the orthopyroxenite 568J and are shown in Fig. 9. They intersect the clinocllore + sapphirine stability field at low pressures and define a narrow *P-T* field for the early mineral assemblages in the Maowu body. Thus, the *P-T* conditions leading to the formation of the clinocllore + talc + sapphirine assemblage were  $730 \pm 30^\circ\text{C}$  and  $4 \pm 2$  kbar assuming unit activity of water, which is plausible for such hydrous mineral assemblages. These *P-T* conditions correspond to those generally associated with amphibolite/granulite-facies boundary and contrast sharply with similar temperatures ( $740^\circ\text{C}$ ) but much higher pressures ( $>40$  kbar) recorded by the matrix minerals.

## Conclusions

The Maowu body has undergone two distinct metamorphic events; an early amphibolite/granulite-facies metamorphism at  $730^\circ\text{C}$  and 4 kbar followed by an ultra-high-pressure metamorphism at  $740^\circ\text{C}$  and above 40 kbar. The Sm-Nd data on eclogites from the Dabie Shan indicate Triassic reworking of an over 1500 million-year-old continental crust (Okay et al. 1993). Thus it is likely that the Dabie Shan Complex was already crystalline before the ultra-high-pressure metamorphism. Granulite-facies relicts are present in the northern zone (Fig. 1, Okay 1993) although they were not found until now in the eclogite zone. Therefore, it is likely that the granulite-facies metamorphism in the Maowu body represents a Precambrian metamorphic event genetically unrelated to the Triassic ultra-high-pressure metamorphism.

The chromium-rich bulk composition of the orthopyroxenites and the metre-scale layering of mafic and ultramafic lithologies suggest that the Maowu body represents part of a crustal, layered-cumulate complex. However, it must have been strongly hydrated before or during the granulite-facies metamorphism. The Maowu body was clearly not a direct mantle fragment as probably is the case for many of the eclogites and associated garnet-peridotites in orogenic belts (cf. Medaris and Carswell 1990).

Eclogites with coesite or with quartz pseudomorphs after coesite occur in the vicinity of the Maowu body (cf. Fig. 1). Although no mineral chemical data are available

from this immediate area, similar coesite-bearing assemblages 15 km north give peak temperatures of about  $800^\circ\text{C}$  and pressures of over 29 kbar (Okay 1993), not dissimilar to those obtained from the Maowu body. If the Maowu body was metamorphosed in place, and not introduced tectonically, then that would imply a regional granulite-facies metamorphism of the eclogite zone prior to the ultra-high-pressure metamorphism.

The case of the Maowu body illustrates that crustal rocks that were metamorphosed at high temperatures at shallow crustal levels can later be subducted to depths of over 150 km and then uplifted to the surface.

*Acknowledgements.* The field work was supported by the Lamont-ITÜ-Oxford Tethyan project and by grants from NNSFC and Anhui Bureau of Geology and Mineral Resources. I thank Xu Shutong and Celal Şengör for assistance during the various stages of this project, Li Buming of the Geological Team 311 from Huangpu for field guidance and Graham Chinner for facilitating the use of the electron probe. Bernard Evans and Jürgen Reinhardt provided detailed reviews of the manuscript.

## References

- Ackermann D, Seifert F, Schreyer W (1975) Instability of sapphirine at high-pressures. *Contrib Mineral Petrol* 50:79–92
- Aoki K, Fujina K, Akaogi M (1976) Titanochondrodite and titanoclinohumite derived from the upper mantle in the Buell Park kimberlite, Arizona USA. *Contrib Mineral Petrol* 56:243–253
- Carswell DA, Gibb FGF (1987) Evaluation of mineral thermometers and barometers applicable to garnet lherzolite assemblages. *Contrib Mineral Petrol* 95:499–511
- Ellis DJ, Green DH (1979) An experimental study of the effect of Ca upon garnet-clinopyroxene Fe-Mg exchange equilibria. *Contrib Mineral Petrol* 71:13–22
- Engi M, Lindsley DH (1980) Stability of titanian clinohumite: experiments and thermodynamic analysis. *Contrib Mineral Petrol* 72:415–424
- Evans BW, Trommsdorff V (1983) Fluorine hydroxyl titanian clinohumite in alpine recrystallised garnet peridotite: compositional controls and petrological significance. *Am J Sci* 283-A: 355–369
- Ghent ED (1988) A review of chemical zoning in eclogite garnets. In: Smith DC (ed) *Eclogites and eclogite-facies rocks*. Elsevier, Amsterdam, pp 207–236
- Harley SL (1984) An experimental study of the partitioning of Fe and Mg between garnet and orthopyroxene. *Contrib Mineral Petrol* 86:359–373
- Higgins JB, Ribbe PH, Herd RK (1979) Sapphirine. I. Crystal chemical contributions. *Contrib Mineral Petrol* 68:349–356
- Holland TJB, Powell R (1990) An enlarged and updated internally consistent thermodynamic dataset with uncertainties and correlations: the system  $\text{K}_2\text{O}-\text{Na}_2\text{O}-\text{CaO}-\text{MgO}-\text{MnO}-\text{FeO}-\text{Fe}_2\text{O}_3-\text{Al}_2\text{O}_3-\text{TiO}_2-\text{SiO}_2-\text{C}-\text{H}_2\text{O}-\text{O}_2$ . *J Metamorphic Geol* 8:89–124
- MacGregor ID (1974) The system  $\text{MgO}-\text{Al}_2\text{O}_3-\text{SiO}_2$ : solubility of  $\text{Al}_2\text{O}_3$  in enstatite for spinel and garnet peridotite compositions. *Am Mineral* 59:110–119
- McGetchin TR, Silver LT, Chodos AA (1970) Titanoclinohumite: A possible mineralogical site for water in the upper mantle. *J Geophys Res* 75:255–259
- Medaris LG, Carswell DA (1990) The petrogenesis of Mg-Cr garnet peridotites in European metamorphic belts. In: Carswell DA (ed) *Eclogite facies rocks*. Blackie, Glasgow, pp 260–290
- Nickel KG, Green DH (1985) Empirical geothermobarometry for garnet peridotites and implications for the nature of the lithosphere, kimberlites and diamonds. *Earth Planet Sci Lett* 73:158–170
- Okay AI (1993) Petrology of a diamond and coesite-bearing metamorphic terrain: Dabie Shan, China. *Eur J Mineral* 5:659–675

- Okay AI, Xu ST, Şengör AMC (1989) Coesite from the Dabie Shan eclogites, central China. *Eur J Mineral* 1:595–598
- Okay AI, Şengör AMC, Satır M (1993) Tectonics of an ultra-high-pressure metamorphic terrane: the Dabie Shan/Tongbai Shan orogen, China. *Tectonics* (in press)
- Perkins III D, Holland TJB, Newton RC (1981) The  $\text{Al}_2\text{O}_3$  contents of enstatite in equilibrium with garnet in the system  $\text{MgO}-\text{Al}_2\text{O}_3-\text{SiO}_2$  at 15–40 kbar and 900–1600°C. *Contrib Mineral Petrol* 78:99–109
- Schreyer W, Abraham K (1975) Peraluminous sapphirine as a metastable reaction product in kyanite-gedrite-talc schist from Sar e Sang, Afghanistan. *Mineral Mag* 40:171–180
- Seifert F (1974) Stability of sapphirine: a study of the aluminous part of the system  $\text{MgO}-\text{Al}_2\text{O}_3-\text{SiO}_2-\text{H}_2\text{O}$ . *J Geol* 82:173–204
- Smith D (1977) Titanochondrodite and titanoclinohumite derived from the upper mantle in the Buell Park kimberlite, Arizona, USA: a discussion. *Contrib Mineral Petrol* 61:213–215
- Staudigel H, Schreyer W (1977) The upper thermal stability of clinocllore  $\text{Mg}_5\text{Al}[\text{AlSi}_3\text{O}_{10}](\text{OH})_8$ , at 10–35 kbar  $P_{\text{H}_2\text{O}}$ . *Contrib Mineral Petrol* 61:187–198
- Trommsdorff V, Evans BW (1980) Titanian hydroxyl-clinohumite: formation and breakdown in antigorite rocks (Malenco, Italy). *Contrib Mineral Petrol* 72:229–242
- Wang X, Liou JG, Mao HK (1989) Coesite-bearing eclogites from the Dabie Mountains in central China. *Geology* 17:1085–1088
- Wang X, Jing Y, Liou JG, Pan G, Liang W, Xia M, Maruyama S (1990) Field occurrences and petrology of eclogites from the Dabie Mountains, Anhui, central China. *Lithos* 25:119–131
- Wells PRA (1977) Pyroxene thermometry in simple and complex systems. *Contrib Mineral Petrol* 62:129–139
- Xu ST, Okay AI, Ji SY, Şengör AMC, Su W, Liu YC, Jiang LL (1992) Diamond from the Dabie Shan metamorphic rocks and its implications for tectonic setting. *Science* 256:80–82

Editorial responsibility: W. Schreyer